



Spectroscopic [IR and Raman] Analysis and Gaussian Hybrid Computational Investigation- NMR, UV-Visible, MEP Maps and Kubo Gap on 2,4,6-Nitrophenol

Ramalingam S^{1*}, John David Ebenezer I², Ramachandra Raja C³ and Jobe Prabakar PC²

¹Department of Physics, A.V.C. College, Mayiladuthurai, Tamilnadu, India

²Department of Physics, TBML College, Porayar, Tamil Nadu, India

³Department of Physics, Government Arts College, Kumbakonam, Tamilnadu, India

Abstract

In the present methodical study, FT-IR and FT-Raman of the 2,4,6-Nitrophenol (TNP) called as picric acid are recorded and the observed vibrational frequencies are assigned. The hybrid computational calculations are carried out by HF and DFT (B3LYP and B3PW91) methods with 6-31+G(d,p) and 6-311++G(d,p) basis sets and the corresponding results are tabulated. The alternation of structure of nitro phenol due to the subsequent substitutions of NO₂ is investigated. The vibrational sequence pattern of the molecule related to the substitutions is analyzed. Moreover, ¹³C NMR and ¹H NMR are calculated by using the gauge independent atomic orbital (GIAO) method with B3LYP methods and the 6-311++G(d,p) basis set and their spectra are simulated and the chemical shifts related to TMS are compared. A study on the electronic properties; absorption wavelengths, excitation energy, dipole moment and frontier molecular orbital energies, are performed by HF and DFT methods. The calculated HOMO and LUMO energies and the kubo gap analysis show that the occurring of charge transformation within the molecule. Besides frontier molecular orbitals (FMO), molecular electrostatic potential (MEP) was performed. NLO properties related to Polarizability and hyperpolarizability are also discussed. The thermodynamic properties (thermal energy, heat capacity and entropy) of the title compound are calculated in gas phase and are interpreted with different types of phenols.

Keywords: 2,4,6-Nitrophenol; Picric acid; First order hyperpolarizability; Vibrational sequence pattern; Chemical shifts; Frontier molecular orbital energies

Introduction

The aromatic systems in conjugated with nitro group leading to charge transfer systems, have been intensely studied and their crystals are highly recognized as the materials of the future because their molecular nature combined with versatility of synthetic chemistry can be used to alter their structure in order to maximize the non-linear properties [1-4]. The nitro substituted phenols with high optical non-linearities are very promising materials for future optoelectronic and non-linear optical applications. The optical transparency of this crystal is quite good and hence it can be a potential material for frequency replication in electro-optic modulation, frequency conversion and THz wave generation of non-linear optics [5,6].

Phenol derivatives are interesting molecules for theoretical studies due to their relatively small size and similarity to biological species. The phenols are organic compounds that contain a hydroxyl group (OH) bound directly to a carbon atom in the benzene ring. The phenol materials with very large second-order nonlinear optical (NLO) susceptibilities have attracted a lot of attention because of their potential applications in electro-optic modulation. The material of phenols with more nitro groups having the properties of large second-order optical nonlinearities, short transparency cut-off wavelength and stable physiochemical performance which are needed in the realization of most of the recent electronic applications. The 2,4,6-Trinitrophenol (TNP), generally known as picric acid, is a nonlinear optical crystal and a well-known organic NLO crystal by its shorter cutoff wavelength, optical quality, sufficiently large nonlinear coefficient, transparency in UV region and high damage threshold [7,8].

Experimental Details

The compound 2,4,6-Trinitrophenol (Picric acid) is purchased from Sigma-Aldrich Chemicals, USA, which is of spectroscopic grade and hence used for recording the spectra as such without any further purification. The FT-IR spectrum of the compound is recorded in Bruker IFS 66V spectrometer in the range of 4000–400 cm⁻¹. The spectral resolution is ± 2 cm⁻¹. The FT-Raman spectrum of same compound is also recorded in the same instrument with FRA 106 Raman module equipped with Nd: YAG laser source operating at 1.064 μm line widths with 200 mW power. The spectra are recorded in the range of 4000-100 cm⁻¹ with scanning speed of 30 cm⁻¹ min⁻¹ of spectral width 2 cm⁻¹. The frequencies of all sharp bands are accurate to ± 1 cm⁻¹.

Computational Calculation

In the present work, HF and some of the hybrid methods; B3LYP and B3PW91 are carried out using the basis sets 6-31+G(d,p) and 6-311+G(d,p). All these calculations have been carried out using GAUSSIAN 09W [9] program package on Pentium IV processor in personal computer. In DFT methods; Becke's three parameter hybrids

***Corresponding author:** Ramalingam S, Department of Physics, A.V.C. College, Mayiladuthurai, Tamilnadu, India, Tel: +91 04364 225367; Fax: +91 04364 225367; E-mail: ramalingam.physics@gmail.com

Received November 26, 2013; **Accepted** January 27, 2014; **Published** February 03, 2014

Citation: Ramalingam S, Ebenezer IJD, Raja CR, Prabakar PCJ (2014) Spectroscopic [IR and Raman] Analysis and Gaussian Hybrid Computational Investigation- NMR, UV-Visible, MEP Maps and Kubo Gap on 2,4,6-Nitrophenol. J Theor Comput Sci 1: 108. doi: [10.4172/2376-130X.1000108](https://doi.org/10.4172/2376-130X.1000108)

Copyright: © 2014 Ramalingam S. This is an open-access article distributed under the terms of the Creative Commons Attribution License, which permits unrestricted use, distribution, and reproduction in any medium, provided the original author and source are credited.

function combined with the Lee-Yang-Parr correlation function (B3LYP) [10,11], Becke's three parameter exact exchange-function (B3) [12] combined with gradient-corrected correlational functional of Lee, Yang and Parr (LYP) [13,14] and Perdew and Wang (PW91) [15,16] predict the best results for molecular geometry and vibrational frequencies for moderately larger molecules. The calculated frequencies are scaled down to yield the coherent with the observed frequencies.

The scaling factors are 0.88 and 0.903 for HF/6-31+G/6-311++G(d,p) method. For B3LYP/6-311++G (d,p) basis set, the scaling factors are 0.980, 0.907, 0.955 and 1.02/0.920, 0.975 and 1.02. For B3PW91/6-31+G/6-311+G (d,p) basis set, the scaling factors are 0.930,0.906, 0.955 and 1.02/0.910, 0.955, 0.982 and 1.02. The optimized molecular structure of the molecule is obtained from Gaussian 09 and Gauss view program and is shown in Figure 1. The comparative optimized

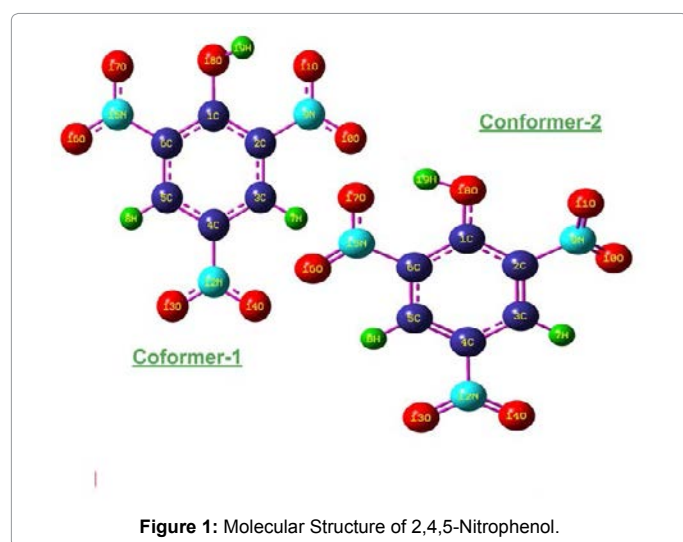


Figure 1: Molecular Structure of 2,4,5-Nitrophenol.

Geometrical Parameters	Methods					Experimental Value
	HF	B3LYP		B3PW91		
	6-311G (d, p)	6-31G (d, p)	6-311G (d, p)	6-31G (d, p)	6-311G (d, p)	
Bond length(A)						
C1-C2	1.408	1.420	1.416	1.418	1.414	1.392
C1-C6	1.410	1.426	1.423	1.424	1.420	1.406
C1-O18	1.299	1.315	1.315	1.310	1.310	1.357
C2-C3	1.371	1.382	1.379	1.380	1.377	1.402
C2-N9	1.458	1.475	1.482	1.470	1.475	1.451
C3-C4	1.385	1.394	1.391	1.392	1.389	1.384
C3-H7	1.071	1.082	1.081	1.083	1.082	1.080
C4-C5	1.371	1.383	1.380	1.381	1.378	1.387
C4-N12	1.451	1.469	1.477	1.464	1.471	1.451
C5-C6	1.384	1.391	1.389	1.389	1.386	1.383
C5-H8	1.070	1.082	1.080	1.083	1.082	1.080
C6-N15	1.449	1.457	1.465	1.451	1.458	1.451
N9-O10	1.194	1.229	1.222	1.224	1.216	1.225
N9-O11	1.186	1.224	1.216	1.218	1.211	1.217
N12-O13	1.192	1.228	1.221	1.223	1.215	1.225
N12-O14	1.191	1.228	1.221	1.222	1.215	1.217
N15-O16	1.183	1.219	1.212	1.214	1.206	1.225
N15-O17	1.206	1.251	1.243	1.245	1.238	1.217
O17-H19	1.782	1.646	1.676	1.625	1.649	-
O18-H19	0.953	0.994	0.987	0.995	0.989	0.820
Bond angle(°)						
C2-C1-C6	115.84	115.83	115.72	115.77	115.64	-
C2-C1-O18	119.31	120.82	120.34	120.97	120.55	-
C6-C1-O18	124.80	123.31	123.91	123.22	123.77	-
C1-C2-C3	122.49	122.08	122.34	122.09	122.35	-
C1-C2-N9	120.81	121.03	120.66	121.01	120.65	-
C3-C2-N9	116.69	116.87	116.99	116.88	116.98	-

C2-C3-C4	119.18	119.41	119.25	119.44	119.28	-
C2-C3-H7	120.03	119.92	120.12	119.90	120.09	-
C4-C3-H7	120.77	120.66	120.62	120.65	120.61	-
C3-C4-C5	121.13	121.47	121.41	121.45	121.38	-
C3-C4-N12	119.43	119.29	119.31	119.29	119.32	-
C5-C4-N12	119.43	119.22	119.26	119.25	119.28	-
C4-C5-C6	119.10	118.67	118.77	118.63	118.73	-
C4-C5-H8	120.82	120.97	120.95	120.98	120.97	-
C6-C5-H8	120.06	120.35	120.26	120.37	120.28	-
C1-C6-C5	122.20	122.50	122.46	122.58	122.55	-
C1-C6-N15	120.85	120.19	120.28	120.08	120.15	-
C5-C6-N15	116.94	117.30	117.25	117.32	117.28	-
C2-N9-O10	116.22	116.35	116.29	116.31	116.26	-
C2-N9-O11	117.98	117.81	117.52	117.67	117.41	-
O10-N9-O11	125.75	125.80	126.15	125.98	126.30	-
C4-N12-O13	117.29	117.24	117.18	117.17	117.12	-
C4-N12-O14	117.16	117.17	117.07	117.08	117.00	-
O13-N12-O14	125.53	125.58	125.74	125.73	125.87	-
C6-N15-O16	118.16	118.95	118.84	118.99	118.91	-
O6-N15-O17	117.89	117.87	117.54	117.72	117.41	-
O16-N15-O17	123.93	123.17	123.60	123.28	123.66	-
C1-O18-H19	110.76	106.52	107.05	106.08	106.42	-
Dihedral angles(°)						
C6-C1-C2-C3	1.466	1.3076	1.149	0.8878	1.151	-
C6-C1-C2-N9	-178.32	-178.85	-178.77	-178.8	-178.7	-
O18-C1-C2-C3	-176.45	-177.36	-177.18	-177.3	-177.1	-
O18-C1-C2-N9	3.7576	2.9185	2.8913	2.9281	2.925	-
C2-C1-C6-C5	-0.0635	0.3338	0.1648	0.3803	0.219	-
C2-C1-C6-N15	-179.74	-179.53	-179.55	-179.4	-179.5	-
O18-C1-C6-C5	177.72	178.516	178.428	178.54	178.46	-
O18-C1-C6-N15	-1.955	-1.3538	-1.2911	-1.331	-1.27	-
C2-C1-O18-H19	178.52	178.269	178.052	178.21	178.04	-
C6-C1-O18-H19	0.8105	0.1744	-0.1351	0.1478	-0.117	-
C1-C2-C3-C4	-2.032	-1.5772	-1.8541	-1.662	-1.923	-
C1-C2-C3-H7	178.18	178.319	177.900	178.24	177.89	-
N9-C2-C3-C4	177.76	178.152	178.075	178.10	178.00	-
N9-C2-C3-H7	-2.014	-1.9507	-2.1694	-1.990	-2.181	-
C1-C2-N9-O10	-145.8	-152.28	-146.70	-151.8	-146.	-
C1-C2-N9-O11	36.250	29.2751	35.0592	29.729	35.55	-
C3-C2-N9-O10	34.382	27.9808	33.3687	28.386	33.86	-
C3-C2-N9-O11	-143.5	-150.45	-144.87	-150.0	-144.3	-
C2-C3-C4-C5	1.1688	1.0898	1.2392	1.178	1.3193	-
C2-C3-C4-N12	-178.9	-179.13	-179.09	-179.0	-179.0	-
H7-C3-C4-C5	-179.0	-178.80	-178.51	-178.7	-178.4	-
H7-C3-C4-N12	0.8001	0.9706	1.1482	1.0071	1.1373	-
C3-C4-C5-C6	0.1782	0.0726	0.026	0.0477	0.0006	-
C3-C4-C5-H8	179.71	179.675	179.622	179.63	179.58	-
N12-C4-C5-C6	-179.6	-179.70	-179.63	-179.6	-179.6	-
N12-C4-C5-H8	-0.132	-0.1012	-0.0404	-0.105	-0.052	-
C3-C4-N12-O13	-179.4	-179.51	-179.32	-179.4	-179.2	-
C3-C4-N12-O14	0.5989	0.4985	0.6989	0.527	0.747	-
C5-C4-N12-O13	0.4134	0.266	0.3458	0.256	0.364	-
C5-C4-N12-O14	-179.5	-179.71	-179.63	-179.7	-179.6	-

C4-C5-C6-C1	-0.729	-0.7932	-0.7334	-0.837	-0.777	-
C4-C5-C6-N15	178.96	179.080	178.994	179.03	178.96	-
H8-C5-C6-C1	179.72	179.601	179.667	179.57	179.63	-
H8-C5-C6-N15	-0.582	-0.5251	-0.6049	-0.547	-0.615	-
C1-C6-N15-O16	-178.4	-178.65	-178.31	-178.64	-178.3	-
C1-C6-N15-O17	1.6025	1.4008	1.7265	1.415	1.743	-
C5-C6-N15-O16	1.8929	1.4677	1.9512	1.477	1.946	
C5-C6-N15-O17	-178.0	-178.47	-178.00	-178.46	-178.0	

Table 1: Optimized geometrical parameters for 2,4,6-Nitrophenol computed at HF/DFT(B3LYP&B3PW91) with 6-31& 6-311G(d, p) basis sets.

structural parameters such as bond length, bond angle and dihedral angle are presented in Table 1. The observed (FT-IR and FT-Raman) and calculated vibrational frequencies and vibrational assignments are submitted in Table 2. Experimental and simulated spectra of IR and Raman are presented in the Figures 2 and 3, respectively.

The ¹H and ¹³C NMR isotropic shielding are calculated with the GIAO method [17] using the optimized parameters obtained from B3LYP/6-311++G(d,p) method. ¹³C isotropic magnetic shielding (IMS) of any X carbon atoms is made according to value ¹³C IMS of TMS,

S.No	Symmetry Species CS	Observed Frequency(cm-1)		Methods					Vibrational Assignments
		FTIR	FTRaman	HF	B3LYP		B3PW91		
					6-311+G (d, p)	6-311+G (d, p)	6-31+G (d, p)	6-311+G (d, p)	
1	A'	3300w	-	3295	3255	3327	3336	3292	(O-H) u
2	A'	2960vs	-	2995	2959	2979	2957	2950	(C-H) u
3	A'	2950vs	-	2988	2955	2975	2954	2946	(C-H) u
4	A'	-	1640vs	1649	1665	1648	1648	1633	(C=C) u
5	A'	-	1630vs	1634	1638	1619	1629	1610	(C=C) u
6	A'	1620vs	-	1616	1622	1632	1617	1597	(C=C) u
7	A'	1550vs	-	1552	1555	1548	1575	1564	(N-O) u as
8	A'	1540vs	-	1540	1539	1531	1561	1551	(N-O) u as
9	A'	-	1475s	1460	1455	1468	1474	1459	(N-O) u as
10	A'	1450vs	-	1449	1452	1432	1426	1455	(C-C) u
11	A'	-	1445vs	1447	1435	1448	1452	1440	(C-C) u
12	A'	-	1440vs	1441	1427	1411	1455	1440	(C-C) u
13	A'	1420vs	-	1420	1416	1398	1443	1429	(N-O) us
14	A'	1340w	1340vs	1324	1336	1351	1317	1344	(N-O) us
15	A'	1310vs	-	1311	1309	1319	1292	1314	(N-O) us
16	A'	1250vs	-	1206	1258	1250	1266	1290	(O-H) δ
17	A'	1180m	-	1185	1175	1187	1157	1180	(C-H) δ
18	A'	-	1150vs	1168	1154	1145	1119	1150	(C-H) δ
19	A'	1090vs	-	1094	1994	1091	1091	1090	(C-N) u
20	A'	1085vs	1085vs	1048	997	995	993	991	(C-N) u
21	A'	950m	-	991	947	960	923	945	(C-N) u
22	A'	-	940m	959	937	950	919	938	(C-O) u
23	A''	-	920vs	941	914	931	903	928	(C-H) γ
24	A''	835m	-	851	840	849	816	845	(C-H) γ
25	A''	830m	830m	828	837	840	809	830	(O-H) γ
26	A'	-	800vs	806	793	809	803	818	(NO2) δ
27	A'	-	795s	785	798	797	807	791	(NO2) δ
28	A'	780vs	-	768	160	760	782	770	(NO2) δ
29	A'	740vs	740s	735	757	744	766	737	(CCC) δ
30	A'	730vs	730vs	725	756	728	761	726	(CCC) δ
31	A'	700vs	700vs	704	733	703	738	714	(CCC) δ
32	A'	-	660w	661	719	688	723	646	(C-N) δ
33	A'	650w	-	647	670	647	673	650	(C-N) δ
34	A'	550w	550w	541	560	548	561	550	(C-N) δ
35	A''	-	530w	525	858	533	516	533	(NO2) γ
36	A''	510w	-	506	515	511	508	514	(NO2) γ
37	A''	420m	-	435	461	410	433	408	(NO2) γ
38	A''	400m	400m	396	412	402	388	403	(CCC) γ
39	A''	360w	-	372	390	349	365	363	(CCC) γ
40	A''	340m	340w	344	355	338	333	342	(CCC) γ
41	A'	330w	-	336	351	332	329	336	(C-O) δ
42	A''	320m	-	322	333	321	312	323	(C-N) γ
43	A''	310m	310w	310	324	310	303	311	(C-N) γ
44	A''	200m	200m	198	207	198	195	199	(C-N) γ

45	A''	190w	-	183	192	188	192	188	(C-O) γ
46	A''	150w	150m	154	158	150	148	153	(C-N) γ
47	A''	120w	-	124	131	121	131	125	(C-N) γ
48	A''	110w	-	88	101	97	102	96	(C-OH) τ
49	A''	105w	-	53	62	60	62	60	(NO ₂) τ
50	A''	100w	100w	52	57	53	57	52	(NO ₂) τ
51	A''	90w	-	49	46	51	46	51	(NO ₂) τ

VS – Very –Strong; S – Strong; m- Medium; w – weak; as- Asymmetric; s – symmetric; u – stretching; δ - In plane bending; γ - out plane bending; τ – Twisting;
Table 2: Observed and HF/DFT (LSDA & B3LYP) with 6-31& 6-311G (d, p) level calculated vibrational frequencies of 2,4,6-Nitrophenol.

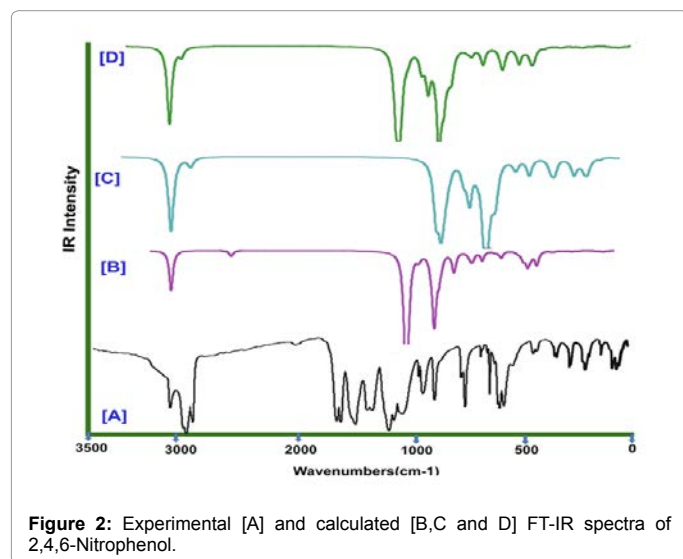


Figure 2: Experimental [A] and calculated [B,C and D] FT-IR spectra of 2,4,6-Nitrophenol.

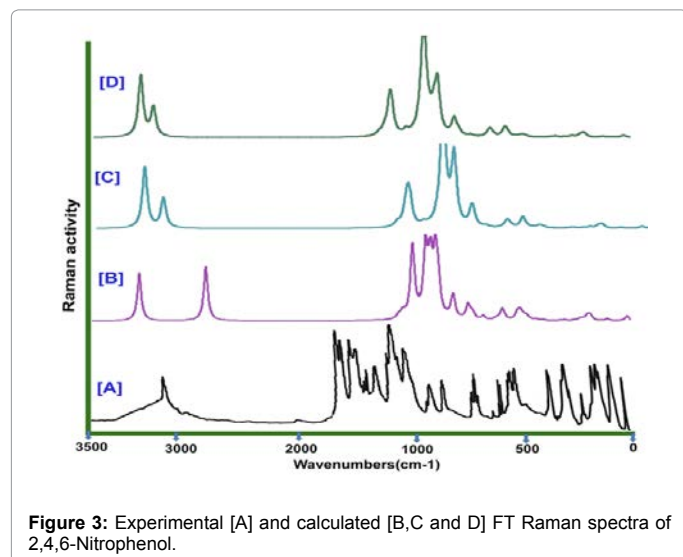


Figure 3: Experimental [A] and calculated [B,C and D] FT Raman spectra of 2,4,6-Nitrophenol.

$CS_x = IMS_{TMS} - IMS_x$. The ¹H and ¹³C isotropic chemical shifts of TMS at B3LYP methods with 6-311++G(d,p) level using the IEFPCM method are calculated for 4-,2,4- and 2,4,6-Nitrophenols. The absolute chemical shift is found between isotropic peaks and the peaks of TMS [18].

The electronic properties, HOMO-LUMO energies, absorption wavelengths and oscillator strengths are calculated using B3LYP method of the time-dependent DFT (TD-DFT) [19,20], basing on the optimized structure in gas phase. Thermodynamic properties of three phenols at 298.15°C have been calculated in gas phase using B3LYP/6-311++G (d,p) method. Moreover, the dipole moment, nonlinear optical

(NLO) properties, linear polarizabilities and first hyperpolarizabilities and chemical hardness have also been studied.

Results and Discussion

Molecular geometry

The molecular structure of TNP belongs to C_s point group symmetry is studied. The optimized two conformers of the molecule is obtained from Gaussian 09 and Gauss view program [12] and is shown in Figure 1 with calculated energies for C_s point group symmetry. The molecule; TNP contains three NO₂ groups along with OH. There is no energy difference between two conformers of title molecule, determined by B3LYP level 6-311++G(d,p). Possible conformers depend on the rotation of O13–H14 bond, linked to C atom. From DFT calculations with 6-311+G(d,p) basis set, the conformer 1 and 2, both are stable.

The structure optimization and zero point vibrational energy of the compound in HF and DFT(B3LYP/B3PW91) with 6-31+/6-311+G(d,p) are 77.77, 70.54, 70.09, 71.09 and 70.69 Kcal/Mol, respectively. The entire calculated values of B3LYP method are greater than the HF method. The breaking of TNP structure belongs to multiple planes which are due to the couple of three NO₂ symmetrically placed about 120° in phenyl ring. The bond length between C-C of the phenyl ring is getting fractured variably. It is also evident from the bond length order as C2-C3<C4-C5<C5-C6<C3-C4<C1-C2<C6-C1. The bond length of C1-C2 and C1-C6 are more elongated than other C-C due to the presence of NO₂ group. The experimental bond length (1.225&1.217 Å) of N-O and C-N are nearly equal to the calculated value (1.224 & 1.218 Å) by B3PW91/6-31G(d,p). The experimental bond length (0.989 Å) of O-H is 0.175 Å greater than calculated value (0.820 Å) by B3PW91/6-31G(d,p).

Vibrational assignments

In order to obtain the spectroscopic signature of the TNP compound, the computational calculations are performed for frequency analysis. The molecule, has C_s point group symmetry, consists of 19 atoms, so it has 51 normal vibrational modes. On the basis of C_s symmetry, the 51 fundamental vibrations of the molecule can be distributed as 32 in-plane vibrations of A' species and 19 out of plane vibrations of A'' species, i.e., $\Gamma_{vib} = 33 A' + 19 A''$. In the C_s group symmetry of molecule is non-planar structure and has the 51 vibrational modes span in the irreducible representations.

The harmonic vibrational frequencies (unscaled and scaled) calculated at HF, B3LYP and B3PW91 levels using the triple split valence basis set along with the diffuse and polarization functions, 6-31+/6-311++G(d,p) and observed FT-IR and FT-Raman frequencies for various modes of vibrations have been presented in Tables 2 and 3. Comparison of frequencies calculated at HF and B3LYP/B3PW91 with the experimental values reveal the over estimation of the calculated vibrational modes due to the neglect of a harmonicity in real system. Inclusion of electron correlation in the density functional theory to

S. No.	Observed frequency	Calculated frequency				
		HF	B3LYP		B3PW91	
		6-311G (d,p)	6-31G (d,p)	6-311G (d,p)	6-31G (d,p)	6-311G (d,p)
1	3300	3972	3289	3360	3271	3325
2	2960	3442	3262	3238	3264	3242
3	2950	3435	3258	3234	3261	3237
4	1640	1895	1699	1682	1726	1710
5	1630	1878	1671	1652	1706	1686
6	1620	1858	1655	1632	1693	1672
7	1550	1784	1628	1613	1649	1638
8	1540	1770	1611	1595	1635	1624
9	1475	1678	1524	1506	1543	1528
10	1450	1647	1482	1469	1493	1482
11	1445	1633	1435	1420	1452	1440
12	1440	1596	1399	1383	1426	1412
13	1420	1572	1388	1371	1415	1401
14	1340	1466	1363	1351	1379	1369
15	1310	1452	1336	1319	1353	1338
16	1250	1336	1317	1302	1326	1314
17	1180	1312	1199	1187	1212	1202
18	1150	1293	1178	1174	1172	1171
19	1090	1212	1094	1091	1092	1090
20	1085	1116	977	975	974	972
21	950	1097	966	960	966	962
22	940	1062	956	950	962	955
23	920	1042	933	931	946	945
24	835	942	840	849	854	860
25	830	917	837	840	847	845
26	800	893	830	809	841	833
27	795	869	782	781	791	791
28	780	851	157	745	767	755
29	740	814	742	744	751	750
30	730	803	741	728	746	739
31	700	780	719	721	724	727
32	660	732	705	706	709	710
33	650	717	657	647	660	650
34	550	599	549	548	550	550
35	530	581	841	533	540	533
36	510	560	505	511	508	514
37	420	482	452	446	453	448
38	400	439	404	402	406	403
39	360	412	382	379	382	380
40	340	381	348	347	349	348
41	330	372	344	340	345	342
42	320	357	326	321	327	323
43	310	343	318	310	317	311
44	200	219	203	198	204	199
45	190	203	188	184	188	184
46	150	171	155	1542	155	153
47	120	137	128	124	128	125
48	110	97	99	95	100	96
49	105	59	61	59	61	59
50	100	58	56	52	56	51
51	90	54	45	50	45	50

Table 3: Calculated unscaled frequencies by HF/DFT (B3LYP&B3PW91) with 6-31(d,p) and 6-311G(d,p) basis sets.

certain extends makes the frequency values smaller in comparison with the HF frequency data. Reduction in the computed harmonic vibrations, although basis set sensitive is only marginal as observed in the DFT values using 6-311+G(d,p).

C-H vibrations: For simplicity, modes of vibrations of aromatic compounds are considered as separate ring C-H or C-C vibrations. However, as with any complex molecules, vibrational interactions occur and these labels only indicate the predominant vibration. Substituted benzenes have large number of sensitive bands, that is, bands whose position is significantly affected by the mass and electronic properties, mesomeric or inductive, of the substituents. According to the literature [21,22], in infrared spectra, most mono nuclear and poly nuclear aromatic compounds have three or four peaks in the region 3000 -3100 cm^{-1} [23], these are due to the stretching vibrations of the ring C-H bonds. Accordingly, in the present study, three C-H stretching vibrations are observed at 2960 and 2950 cm^{-1} . These assigned frequencies are shifted down to the observed region which is strongly indicates that the ring vibrations affected much by the substitutions. The C-H in-plane and out-of-plane bending vibrations generally lies in the range 1000-1300 cm^{-1} and 950 - 800 cm^{-1} [24-26] respectively. Three C-H in-plane bending vibrations are identified at 1180 and 1150 cm^{-1} and three C-H out-of-plane bending vibrations are observed at 835 and 830 cm^{-1} . According to the literature, the in-plane and out-of-plane bending vibrational frequencies are found to be well within their characteristic regions.

CC vibrations: Generally, the C=C stretching vibrations in aromatic compounds are seen in the region of 1430-1650 cm^{-1} [27-29]. The C=C stretching vibrations of TNP are observed with very strong intensity at 1640, 1630 and 1620 cm^{-1} . The stretching vibrational bands for C-C bond are observed at 1450, 1445 and 1440 cm^{-1} . All bands lie in the lower end of the expected range when compared to the literature values. The CCC in-plane bending vibrations are observed at 740, 730 and 700 cm^{-1} and the out-of-plane bending vibrations are appeared at 400, 360 and 340 cm^{-1} . These assignments are in good agreement with the literature [30,31].

NO₂ vibrations: Aromatic nitro compounds have strong absorptions due to asymmetric and symmetric stretching vibrations of the NO₂ group at 1570 -1485 and 1370-1320 cm^{-1} , respectively, Hydrogen bonding has a little effect on the NO₂ asymmetric stretching vibrations [32,33]. In the present case, very strong bands at 1550, 1540 and 1475 cm^{-1} and 1420, 1340 and 1310 cm^{-1} have been assigned to asymmetric and symmetric stretching modes of NO₂. Each one of the stretching vibrations is moved down from the expected region. This realignment of the vibrations is purely due to the inductive effect of O of NO₂ and H of Phenol. Aromatic nitro compounds have a band of weak to medium intensity in the region 590 - 500 cm^{-1} [34] due to the out of plane bending deformations mode of NO₂ group. This is observed with strong intensity at 530, 510 and 420 cm^{-1} for the title compound. The in plane NO₂ deformation vibrations have a weak to medium absorption in the region 775-660 cm^{-1} [35,36]. In the present case, the NO₂ deformation is found at 800, 795 and 780 cm^{-1} . The NO₂ twisting vibrations are observed at 105, 100 and 90 cm^{-1} . One band of in plane bending pushed up and one band of out of plane bending pulled down. This is mainly due to OH.

C-N vibrations: The C-N stretching signal is raised in the region of 1350-1000 cm^{-1} [37]. In the present compound, the C-N stretching vibrations are observed at 1090, 1085 and 950 cm^{-1} . The C-N bending vibrations of a nitro group take place around 870 and 610 cm^{-1} , respectively [38]. The C-N in-plane bending of a nitro group for the title compound assigned at 660, 650 and 550 cm^{-1} , respectively. The C-N out-of-plane bending vibrations are found at 320, 310 and 200 cm^{-1} . Some of the assigned values of C-N stretching and bending vibrations are observed at out of the expected region. The repulsion between the NO₂ reduce the wavenumber of normal mode of vibrations.

C-O and O-H vibrations: The TNP compound contain a carbonyl group, the absorption caused by the C-O stretching is generally very strong [39]. Consideration of these factors lead to assign a band observed at 940 cm^{-1} to C-O stretching vibration. The in-plane bending and out-of-plane bending vibrations appear at 330 cm^{-1} and 190 cm^{-1} respectively. Also a weak band is observed at 110 cm^{-1} for C-OH twisting vibration. From the above observation, it is clear that the assigned band is in the expected region [40] and in good agreement with computed values at B3LYP/6-311+G(d,p).

The OH group gives rise to three vibrations, stretching, in-plane bending and out of plane bending vibrations. The OH group vibrations are likely to be the most sensitive to the environment, so they show pronounced shifts in the spectra of the hydrogen-bonded species. The O-H stretching vibrations are sensitive to hydrogen bonding. The O-H stretching vibration is normally observed around 3300 cm^{-1} [41]. Accordingly, in TNP, the O-H stretching is found at 3300 cm^{-1} . The O-H in-plane and out-of-plane bending vibrations are usually observed in the regions $1350\text{-}1200\text{ cm}^{-1}$ and $720\text{-}590\text{ cm}^{-1}$ [42,43], respectively. The O-H in-plane and out-of-plane bending vibrations are found at 1250 cm^{-1} and 830 cm^{-1} , respectively. Except one, the assignment is in line with the literature. The out of plane bending vibration is shifted up to the higher region which is may be favor of NO_2 .

NMR examination

NMR spectroscopy is currently used for structure elucidation of organic molecules. The combined use of experimental and computational methods offers a powerful tool to interpret and predict the structure of bulky molecules. The optimized structure of TNP is used to calculate the NMR spectra at B3LYP method with 6-311++G(d,p) level using the GIAO method and the chemical shifts of the compound are reported in ppm relative to TMS for ^1H and ^{13}C NMR spectra which are presented in Tables 4 and 5. The corresponding spectra are shown in Figure 4.

In view of the range of ^{13}C NMR chemical shifts for similar organic molecules usually is $>100\text{ ppm}$ [44,45], the accuracy ensures reliable

Atom position	Solvent-DMSO		Shift
	B3LYP/6-311+G(d,p) (ppm)	B3LYP/6-311+G(2d,p) GIAO (ppm)	
C1	11.04	188.94	177.9
C2	40.02	159.95	119.93
C3	44.60	155.38	110.78
C4	35.61	164.36	128.75
C5	45.30	154.68	109.38
C6	38.84	161.13	122.29
N9	142.52	400.92	258.4
N12	143.74	402.14	258.4
N15	144.99	403.39	258.4
O10	358.20	678.20	320
O11	419.78	739.78	320
O13	354.19	674.19	320
O14	354.47	674.47	320
O16	385.78	695.88	310.1
O17	331.81	651.81	320
O18	171.58	148.42	23.16
H7	22.59	9.29	13.3
H8	22.70	9.18	13.52
H19	22.03	8.84	13.19

Table 4: Experimental and calculated ^1H and ^{13}C NMR chemical shift (ppm) of 2,4,6,-Nitrophenol.

interpretation of spectroscopic parameters. In the present work, ^{13}C NMR chemical shifts in the ring are $>100\text{ ppm}$, as they would be expected (Table 5).

In the case of 4-Nitrophenol, the chemical shift of C1 and C4 are 165 and 117 ppm respectively. The shift is more in C1 and C4 than rest of others. This is mainly due to the substitutions of OH and NO_2 . The shift of H13 is 24.33 ppm which is greater than other which is purely due to O. In the case of 2,6-Nitrophenol, the chemical shift of C1, C2 and C6 are 149, 102 and 104 ppm respectively. The shift is more in C1, C2 and C6 than rest of others. This is mainly by OH and NO_2 .

In the case of 2,4,6-Nitrophenol, three nitro groups are added to the phenyl ring. The N atom has the most electronegative property which polarizes the electron distribution in its bond to adjacent carbon atom and thus increases the chemical shift of C1, C2, C4 and C6 (164, 100, 105 and 103 ppm respectively). The shift is more in C1, C2 and C6 than rest of others in the ring. This is also mainly due to the substitutions of OH and NO_2 on C1, C2 and C6. Thus, the chemical shift of C1, C2 and C6 in the ring is increased by breaking of proton shield due to the substitutions of NO_2 . The shift of other C in the ring is fluctuated depending upon the positions of the NO_2 . The chemical shifts of all C are decreased in going from nitro to tri-nitro phenol. The chemical shift of O of phenol is decreased (73.01, 46.37 and 7.25 ppm) abruptly from nitro to tri-nitro since the isolation of O-H. This effect of isolation is the main cause to change the chemical property from nitro phenol to tri-nitro phenol. There is no change of chemical shift in N and O between three phenols. This view shows that the rigidity of the diamagnetic shielding of the atom. From the observation, it is clear that the change of chemical property of phenols is only in favor of NO_2 groups. In addition to that, due to the accessibility of nitro groups, the phenyl ring itself is disrupted. This view is also evident that the entire property of the phenol is deflected towards nitro group.

Electronic properties-HOMO-LUMO analysis

The frontier molecular orbitals are very much useful for studying the electric and optical properties of the organic molecules. The stabilization of the bonding molecular orbital and destabilization of the antibonding can increase when the overlap of two orbitals increases. In the molecular interaction, there are the two important orbitals that interact with each other. One is the highest energy occupied molecular orbital is called HOMO represents the ability to donate an electron. The other one is the lowest energy unoccupied molecular orbital is called LUMO as an electron acceptor. These orbitals are sometimes called the *frontier* orbitals. The interaction between them is much stable and is called filled empty interaction.

The 3D plots of the frontier orbitals, HOMO and LUMO for TNP molecule are in gas, shown in Figures 5 and 6. According to Figure 5, the HOMO is mainly localized over three carbons of phenyl ring which connects two NO_2 groups. The SP orbital lobe of O-H overlapped with SP of O of nearby NO_2 group. However, LUMO is characterized by a charge distribution on carbons of phenyl ring and nitrogen of NO_2 groups. When the two same sign orbitals overlap to form a molecular orbital, the electron density will occupy at the region between two nuclei. The molecular orbital resulting from in-phase interaction is defined as the bonding orbital which has lower energy than the original atomic orbital. The out of phase interaction forms the anti bonding molecular orbital with the higher energy than the initial atomic orbital. From this observation it is clear that the in and out of phase interaction are present in HOMO and LUMO respectively. The HOMO→LUMO

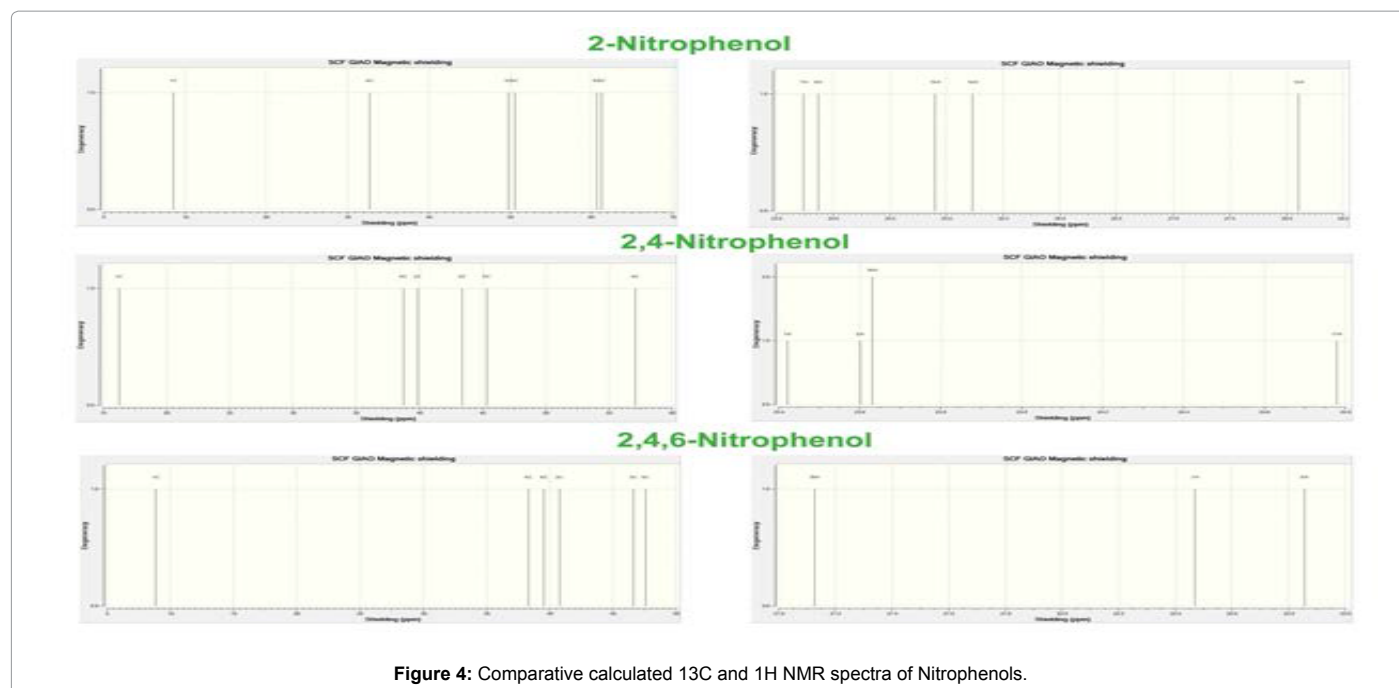


Figure 4: Comparative calculated ^{13}C and ^1H NMR spectra of Nitrophenols.

Atom position	B3LYP/6-311+G(d,p) (ppm)	TMS B3LYP/6-311+G(2d,p) GIAO (ppm)	Shift (ppm)	B3LYP/6-311+G(d,p) (ppm)	TMS B3LYP/6-311+G(2d,p) GIAO (ppm)	Shift (ppm)	B3LYP/6-311+G(d,p) (ppm)	TMS B3LYP/6-311+G(2d,p) GIAO (ppm)	Shift (ppm)
4-Nitrophenol			2,6-Nitrophenol			2,4,6-Nitrophenol			
C1	8.61	173.84	165.23	16.23	166.22	149.99	8.838	173.62	164.78
C2	61.28	121.17	59.89	39.87	142.58	102.71	40.77	141.68	100.91
C3	49.78	132.67	82.89	43.39	139.06	95.67	46.62	135.84	89.22
C4	32.70	149.75	117.05	57.09	125.37	68.28	38.32	144.13	105.81
C5	50.59	131.87	81.28	45.32	137.14	91.82	47.57	134.89	87.32
C6	60.71	121.75	61.04	38.75	143.71	104.96	39.53	142.92	103.39
N9	144.60	403.00	258.4	140.59	398.99	258.4	135.74	394.14	258.40
N12	-	-	-	144.66	403.06	258.4	138.40	396.80	258.40
N15	-	-	-	-	-	-	141.99	400.39	258.40
O10	351.77	671.77	320	367.36	687.36	320	370.92	690.92	320.0
O11	353.39	673.39	320	452.81	772.81	320	448.08	768.08	320.0
O13	-	-	-	384.59	704.59	320	371.00	693.00	322.0
O14	-	-	-	336.58	656.58	320	374.94	694.93	319.0
O16	-	-	-	-	-	-	400.21	720.21	320.0
O17	-	-	-	-	-	-	315.40	635.40	320.0
O18(12)(15)	196.50	123.49	73.01	183.18	136.81	46.37	156.37	163.62	7.25
H7	23.73	8.14	15.59	23.42	8.46	14.96	22.46	9.41	13.05
H8	23.87	8.01	15.86	23.60	8.28	15.32	22.85	9.02	13.83
H13	28.10	3.77	24.33	-	-	-	-	-	-
H14	25.22	6.65	18.57	-	-	-	-	-	-
H15	24.90	6.98	17.92	-	-	-	-	-	-
H16	-	-	-	23.63	8.25	15.38	-	-	-
H17	-	-	-	24.77	7.10	16.67	-	-	-
H19	-	-	-	-	-	-	21.12	10.75	10.37

Table 5: Experimental and calculated ^1H and ^{13}C NMR chemical shift (ppm) of 2,4,6,-Nitrophenol.

transition implies an electron density transfer from NO_2 groups. The HOMO and LUMO energy are 8.408 eV and 4.053 eV in gas phase (Figure 5). Energy difference between HOMO and LUMO orbital is called as energy gap (kubo gap) that is an important stability for

structures. The DFT level calculated energy gap is 4.355 eV, show the lowering of energy gap and reflect the moderate electrical activity of the molecule.

Optical properties (HOMO-LUMO analysis)

The UV and visible spectroscopy is used to detect the presence of chromophores in the molecule and whether the compound has NLO properties or not. The calculations of the electronic structure of TNP are optimized in singlet state. The low energy electronic excited states of the molecule are calculated at the B3LYP/6-311++G (d,p) level using the TD-DFT approach on the previously optimized ground-state geometry of the molecule. The calculations are performed for 2-, 2,6-,

2,4,6-Nitrophenols with gas phase. The calculated excitation energies, oscillator strength (f) and wavelength (λ) and spectral assignments are given in Table 6. The major contributions of the transitions are designated with the aid of SWizard program [46]. TD-DFT calculations predict three transitions in the near Visible and quartz ultraviolet region for TNP molecule. In the case of 2-Nitrophenol, the strong transition is at 279.57 nm with an oscillator strength $f=0.247$. In the case of 2,6-Nitrophenol, strong transition is at 330.87 nm with an oscillator strength $f=0.057$, In the case of 2,4,6-Nitrophenol strong transition is at 418.51 nm with an oscillator strength $f=0.001$ assigned to an $n \rightarrow \pi^*$ transition. This shows that, the transitions moved from quartz ultraviolet to visible region. This view indicates that, the TNP molecule colored and it is capable of having rich NLO properties. In view of calculated absorption spectra, the maximum absorption wavelength corresponds to the electronic transition from the HOMO to LUMO with maximum contribution. In this present compound, the chromophores is NO_2 group, the properties are changed and enhanced from nitro phenol to tri-nitro phenol by adding NO_2 group further.

ISSN: 2376-130X, an open access journal

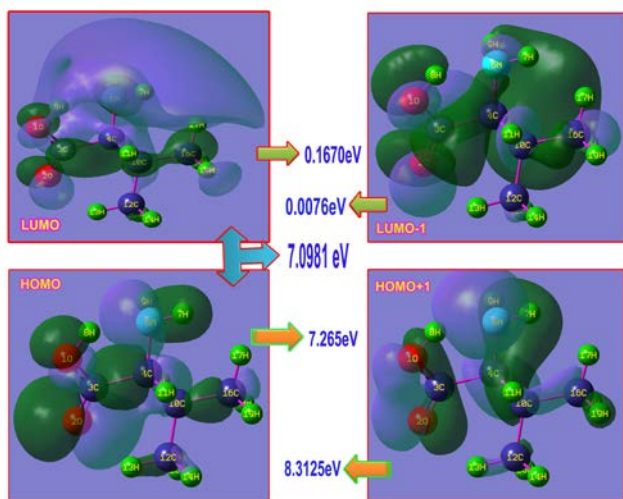


Figure 5: Frontier Molecular Orbitals, Homo and Lumo for 2,4,6-Nitrophenol(Picric acid).

The chemical hardness and potential, electronegativity and Electrophilicity index are calculated and their values are shown in Table 7. The chemical hardness is a good indicator of the chemical stability. The chemical hardness is decreased slightly (2.381-2.033) in going from nitro to tri nitro phenols. Hence, the present compound has much chemical stability. Similarly, the electronegativity is increased from 2.63 up to 3.315, if the value is greater than 1.7; the property of bond is changed from covalent to ionic. Accordingly, the bonds in the compound converted from covalent to ionic. Electrophilicity index is a measure of energy lowering due to maximal electron flow between donor [HOMO] and acceptor [LUMO]. From the Table 6, it

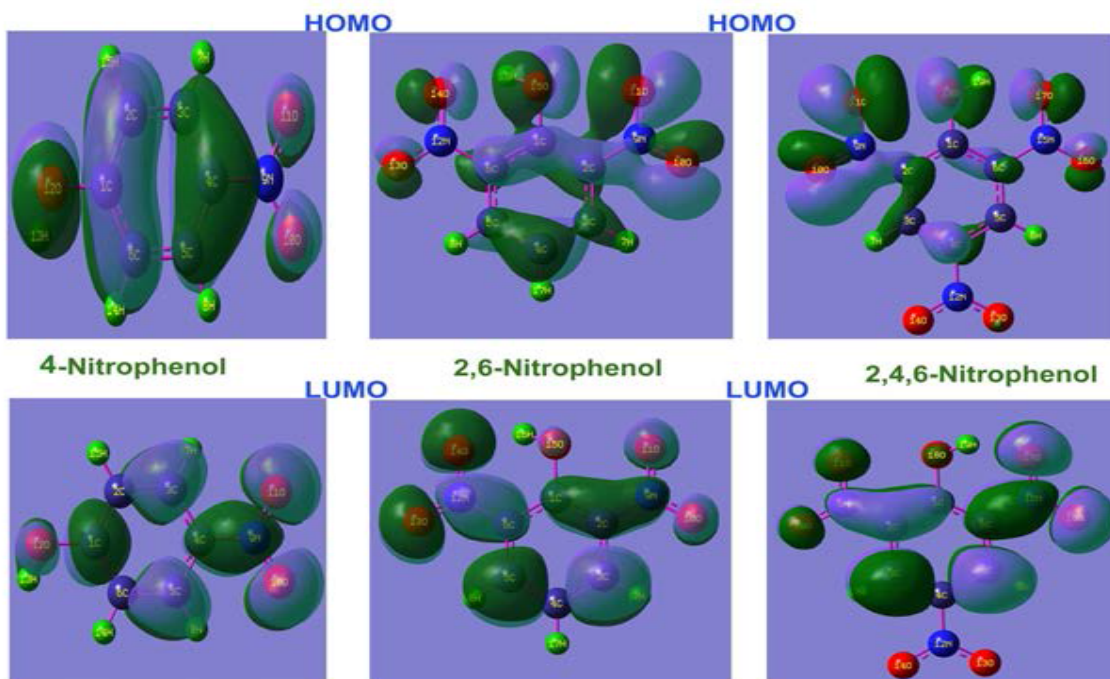


Figure 6: Frontier Molecular Orbitals, Homo and Lumo between Nitrophenols.

TD-DFT/B3LYP/6-311G++(d,p)	2-Nitrophenol	2,6-Nitrophenol	2,4,6-Nitrophenol
E_{total} (Hartree)	512.10	534.23	568.59
E_{HOMO} (eV)	7.447	7.809	8.363
E_{LUMO} (eV)	2.683	3.680	4.296
$\Delta E_{HOMO-LUMO}$ gap (eV)	4.763	4.129	4.067
E_{HOMO-1} (eV)	7.856	8.133	8.865
E_{LUMO+1} (eV)	1.329	3.001	3.910
$\Delta E_{HOMO-1-LUMO+1}$ gap (eV)	6.527	5.132	4.955
Chemical hardness (η)	2.381	2.064	2.033
Electronegativity (χ)	2.632	2.985	3.315
Chemical potential (μ)	-5.065	-5.744	-6.329
Chemical softness(S)	0.419	0.484	0.491
Electrophilicity index (ω)	5.387	7.476	9.851
Dipole moment	5.065	4.896	1.837

Table 6: Calculated energy values, chemical hardness, electro negativity, Chemical potential and Electrophilicity index of 2,4,6-Nitrophenol in Gas phase from UV-Visible.

2-Nitrophenol			Gas	Assignment	Region
λ (nm)	E (eV)	(f)	Major contribution		
279.57	4.434	0.247	L→H+1 (90%)	$n \rightarrow \pi^*$	Quartz UV
274.66	4.514	0.012	L→H+1 (88%)	$n \rightarrow \pi^*$	Quartz UV
224.92	5.512	0.033	H→L-1 (92%)	$n \rightarrow \pi^*$	Quartz UV
2,6-Nitrophenol					
330.87	3.747	0.057	H→L (94%)	$\pi \rightarrow \pi^*$	Quartz UV
319.78	3.877	0.016	H→L (93%)	$\pi \rightarrow \pi^*$	Quartz UV
305.49	4.058	0.007	H→L (86%)	$n \rightarrow \pi^*$	Quartz UV
291.39	4.255	0.004	H→L (86%)	$n \rightarrow \pi^*$	Quartz UV
2,4,6-Nitrophenol					
418.51	2.962	0.001	H→L (86%)	-	Visible
374.54	3.310	0.001	H→L (86%)	$n \rightarrow \pi^*$	Quartz UV
370.89	3.342	0.00	H→L (86%)	$n \rightarrow \pi^*$	Quartz UV

H: HOMO; L: LUMO

Table 7: Electronic absorption spectra of 2,4,6-Nitrophenol (absorption wavelength λ (nm), excitation energies E (eV) and oscillator strengths (f) using TD-DFT/B3LYP/6-311++G(d,p) method gas phase.

is found that the Electrophilicity index of TNP is 9.851, which is too high when compared with other two molecules and this value ensure that the strong energy transformation between HOMO and LUMO. The dipole moment in a molecule is another important electronic property. Whenever the molecule has larger the dipole moment, the intermolecular interactions are very strong. The calculated dipole moment value for the title compound is 1.837 Debye. It is very low when compared to other two nitro phenols. Therefore, it is concluded that, the TNP has weak intermolecular interactions.

Molecular electrostatic potential (MEP) map

The molecular electrical potential surfaces illustrate the charge distributions of molecules three dimensionally. This map allows us to visualize variably charged regions of a molecule. Knowledge of the charge distributions can be used to determine how molecules interact with one another and it is also be used to determine the nature of the chemical bond. Molecular electrostatic potential is calculated at the B3LYP/6-311+G (d,p) optimized geometry. There is a great deal of intermediary potential energy, the non red or blue regions indicate that the electro negativity difference is not very great. In a molecule with a great electro negativity difference, charge is very polarized, and there are significant differences in electron density in different regions of the molecule. This great electro negativity difference leads to regions

that are almost entirely red and almost entirely blue. Greater regions of intermediary potential, yellow and green, and smaller or no regions of extreme potential, red and blue, are key indicators of a smaller electronegativity.

The color code of these maps is in the range between -0.0472 a.u. (deepest red) to 0.0472 a.u. (deepest blue) in compound. The positive (blue) regions of MEP are related to electrophilic reactivity and the negative (green) regions to nucleophilic reactivity shown in Figure 7. As can be seen from the MEP map of the title molecule, the negative regions are mainly localized on the oxygen atoms. A maximum positive region is localized on the carbon and nitrogen atoms indicating a possible site for nucleophilic attack. The MEP map shows that the negative potential sites are on electronegative atoms (O atom) as well as the positive potential sites are around the carbon and nitrogen atoms. From these results, it is clear that the carbon and nitrogen atoms indicate the strongest attraction and O atom indicates the strongest repulsion.

Polarizability and first order hyperpolarizability calculations

In order to investigate the relationships among molecular structures and non-linear optic properties (NLO), the polarizabilities and first order hyperpolarizabilities of the TNP compound was calculated using DFT-B3LYP method and 6-311+G (d,p) basis set, based on the finite-field approach.

The polarizability and hyperpolarizability tensors ($\alpha_{xx}, \alpha_{xy}, \alpha_{yy}, \alpha_{xz}, \alpha_{yz}, \alpha_{zz}$ and $\beta_{xxx}, \beta_{xxy}, \beta_{xyy}, \beta_{yyy}, \beta_{xxz}, \beta_{xyz}, \beta_{yyz}, \beta_{xzz}, \beta_{yzz}, \beta_{zzz}$) can be

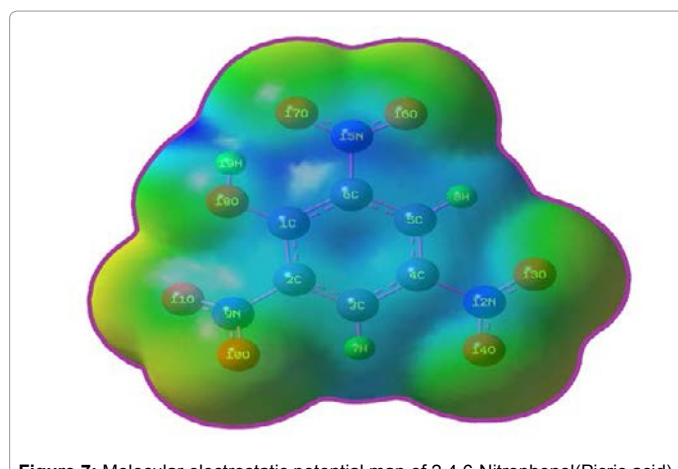


Figure 7: Molecular electrostatic potential map of 2,4,6-Nitrophenol(Picric acid).

Parameter	a.u.	Parameter	a.u.
α_{xx}	104.40	β_{xxx}	-62.31
α_{xy}	3.88	β_{xxy}	-6.533
α_{yy}	105.65	β_{yyy}	22.382
α_{xz}	1.304	β_{yyz}	-4.513
α_{yz}	0.627	β_{xzz}	-5.928
α_{zz}	13.88	β_{yzz}	4.527
α_{tot}	149.96	β_{zzz}	5.120
$\Delta\alpha$	288.01	β_{tot}	-0.109
μ_x	-0.903	β_{zzz}	-3.914
μ_y	1.540	β_{zzz}	0.0087
μ_z	0.0491	β_{tot}	129.66
μ	1.786		

Table 8: The dipole moments μ (D), the Polarizability α (a.u.), the average Polarizability α_0 (esu), the anisotropy of the Polarizability $\Delta\alpha$ (esu), and the first hyperpolarizability β (esu) of 2,4,6-Nitrophenol.

Compound	$C_{p,m}^0$ (calmol ⁻¹ K ⁻¹)	S_m^0 (calmol ⁻¹ K ⁻¹)	ΔH_m^0 (kcalmol ⁻¹)
2-Nitrophenol	27.86	83.32	4.712
2,4-Nitrophenol	35.65	78.73	5.236
2,4,6-Nitrophenol	43.25	85.18	5.549

Table 9: Thermodynamic properties at different temperatures on the B3LYP/6-311+G(d,p) level for Nitrophenols.

obtained by a frequency job output file of Gaussian. However, α and β values of Gaussian output are in atomic units (a.u.) so they have been converted into electronic units (esu) (α 1 a.u.=0.1482 \times 10⁻²⁴ esu, β ; 1 a.u.=8.6393 \times 10⁻³³ esu). The mean polarizability (α), anisotropy of polarizability ($\Delta\alpha$) and the average value of the first hyperpolarizability $\langle\beta\rangle$ can be calculated using the equations.

$$\alpha_{tot} = \frac{1}{3}(\alpha_{xx} + \alpha_{yy} + \alpha_{zz}) \quad (1)$$

$$\Delta\alpha = \frac{1}{\sqrt{2}}[(\alpha_{xx} - \alpha_{yy})^2 + (\alpha_{yy} - \alpha_{zz})^2 + (\alpha_{zz} - \alpha_{xx})^2 + 6\alpha_{xz}^2 + 6\alpha_{xy}^2 + 6\alpha_{yz}^2]^{1/2} \quad (2)$$

$$\langle\beta\rangle = [(\beta_{xxx} + \beta_{yyy} + \beta_{zzz})^2 + (\beta_{yyy} + \beta_{zzz} + \beta_{xxx})^2 + (\beta_{zzz} + \beta_{xxx} + \beta_{yyy})^2]^{1/2} \quad (3)$$

In Table 8, the calculated parameters described above and electronic dipole moment $\{\mu_i$ (i=x, y, z) and total dipole moment μ_{tot} for title compound are listed. The total dipole moment is calculated using the following equation

$$\mu_{tot} = (\mu_x^2 + \mu_y^2 + \mu_z^2)^{1/2} \quad (4)$$

It is well known that, molecule with high values of dipole moment, molecular polarizability, and first hyperpolarizability having more active NLO properties. The first hyperpolarizability (β) and the component of hyperpolarizability β_x , β_y and β_z of TNP along with related properties (μ_0 , α_{total} , and $\Delta\alpha$) are reported in Table 8. The calculated value of dipole moment is found to be 1.837 Debye. The highest value of dipole moment is observed for component μ_x . In this direction, this value is equal to 1.54 D. The lowest value of the dipole moment of the TNP compound is μ_z component (0.049 D). The calculated average Polarizability and anisotropy of the Polarizability is 149.96 \times 10⁻²⁴ esu and 288.01 \times 10⁻²⁴ esu, respectively. The magnitude of the molecular hyperpolarizability β , is one of important key factors in a NLO system. The B3LYP/6-311+G(d,p) calculated first hyperpolarizability value (β) is 129.66 \times 10⁻³⁰ esu. From the above results, it is observed that, the molecular Polarizability and hyperpolarizability of the title compound in all coordinates are active. So that, the TNP can be used to prepare NLO crystals and those crystal is able to produce second order harmonic waves.

Thermodynamic properties

The values of some thermodynamic parameters; thermal energy, specific heat capacity, rotational constants and entropy calculated by B3LYP with 6-311+G(d,p) method at 298.15 K and 1.00 Atm pressure are listed in the Table 9. The variation of thermo dynamical parameters seems to be important because the entire chemical, electrical and thermal properties of the compound depend upon these factors. The specific heat capacity of the TNP is 85.18 cal/mol/K, which is greater than other two phenols. When the number of NO₂ is added, the specific heat capacity of the phenols is increased. Therefore, TNP in crystal form has electrical property and can be used for many industrial applications. Similarly, the values of thermal energy and entropy of TNP is higher than rest of other. From this observation, it is inferred that, the TNP has good chemical reactivity according to the second law of thermodynamics in thermo chemical field.

Conclusion

In the present investigation, FT-IR and FT-Raman spectra of the 2,4,6-Nitrophenol were recorded and the observed vibrational frequencies were assigned depending upon their expected region. The hybrid computational calculations were carried out by HF and DFT (B3LYP and B3PW91) methods with 6-31+G(d,p) and 6-311++G(d,p) basis sets and the corresponding results were tabulated. The alternation of structure and some of the parameters of nitro phenol due to the subsequent substitutions of NO₂ was investigated. The vibrational sequence pattern of the molecule related to the substitutions was analyzed. Moreover, ¹³C NMR and ¹H NMR were calculated by using the gauge independent atomic orbital (GIAO) method with B3LYP methods and the 6-311++G(d,p) basis set and their spectra were simulated and the chemical shifts related to TMS were compared. A study on the electronic properties; absorption wavelengths, excitation energy, dipole moment and frontier molecular orbital energies, were performed by HF and DFT methods. The calculated HOMO and LUMO energies and the Kubo gap analysis show that the occurring of charge transformation within the molecule. Besides frontier molecular orbitals (FMO), molecular electrostatic potential (MEP) was performed. NLO properties related to Polarizability and hyperpolarizability was also discussed. The thermodynamic properties (thermal energy, heat capacity and entropy) of the title compound are calculated in gas phase and were interpreted with different types of phenols.

References

- Chemla DC, Zyss J (1987) Nonlinear Optical Properties of Organic Molecules and Crystals, vol. 1–2, Academic Press, Orlando, Florida, USA.
- Vijayan N, Ramesh Babu R, Gopalakrishnan R, Ramasamy P, Harrison WTA (2004) Growth and characterization of benzimidazole single crystals: a nonlinear optical material. J Cryst Growth 262: 490-498.
- Goto Y, Hyashi A, Kimura Y, Nakayama SM (1991) Second harmonic generation and crystal growth of substituted thienylchalcone. J Cryst Growth 108: 688-698.
- Arivazhagan M, Jeyavijayan S (2011) Vibrational spectroscopic, first-order hyperpolarizability and HOMO, LUMO studies of 1,2-dichloro-4-nitrobenzene based on Hartree-Fock and DFT calculations. Spectrochimica Acta Part A 79: 376-383.
- Schneider A, Neis M, Stillhart M, Ruiz B, Khan R U A, Gunter P (2006) Generation of terahertz pulses through optical rectification in organic DAST crystals: theory and experiment. J Opt Soc Am B 23: 1822-1835.
- Ferguson B, Zhang XC (2002) Materials for terahertz science and technology. Nat Mater 1: 26-33.
- Srinivasan P, Gunasekaran M, Kanagasekaran T, Gopalakrishnan R (2006) J Cryst Growth 289: 639-646
- Hong Zhang, Fang Chen, Feng Zhao, Chuan-Min Meng (2008) Structural and electronic properties of 2,4,6-trinitrophenol. J Mol Struct: THEOCHEM 857: 33-37.
- Frisch MJ (2009) Gaussian 09, Revision A.1, Gaussian, Inc., Wallingford CT.
- Zhengyu Z, Dongmei D J (2000) Calculation of the energy of activation in the electron transfer reaction not involving the bond rupture at the electrode. Mol Struct (Theochem) 505: 247-252.
- Zhengyu Z, Aiping F, Dongmei (2000) Studies on density functional theory for the electron-transfer reaction mechanism between M-C6H6 and M+-C6H6 complexes in the gas phase. D J Quant Chem 78: 186-189.
- Becke AD (1988) Density-functional exchange-energy approximation with correct asymptotic behavior. Phys Rev A 38: 3098-3100.
- Lee C, Yang W, Parr RG (1988) Development of the Colle-Salvetti correlation-energy formula into a functional of the electron density. Phys Rev B Condens Matter 37: 785-789.
- Becke AD (1993) J Chem Phys 98: 5648-5652.

15. Perdew JP, Burke K, Wang Y (1996) Generalized gradient approximation for the exchange-correlation hole of a many-electron system. *Phys Rev B Condens Matter* 54: 16533-16539.
16. Young DC (2001) *Computational Chemistry: A Practical guide for applying Techniques to Real world Problems* John Wiley and Sons Inc., New York, USA.
17. Wolinski K, Hinton JF, Pulay P (1990) Efficient implementation of the gauge-independent atomic orbital method for NMR chemical shift calculations. *J Am Chem Soc* 112: 8251-8260.
18. Cheeseman JR, Trucks GW, Keith TA, Frisch MJ (1996) *J Chem Phys* 104: 5497-5509.
19. Runge E, Gross EKH (1984) Density-Functional Theory for Time-Dependent Systems. *Physics Review Letters*, 52: 997-1000.
20. Bauernschmitt R, Ahlrichs R (1996) Treatment of electronic excitations within the adiabatic approximation of time dependent density functional theory. *Chem Phys Lett* 256: 454-464.
21. Socrates G (1996) *Infrared and Raman Characteristic group frequencies*, 3rd edition, Wiley, New York, USA.
22. Eazhilarasi G, Nagalakshmi R, Krishnakumar V (2008) Studies on crystal growth, vibrational and optical properties of organic nonlinear optical crystal: p-aminoazobenzene. *Spectrochim Acta A Mol Biomol Spectrosc* 71: 502-507.
23. Varsanyi G (1974) *Assignments of Vibrational Spectra of Seven Hundred Benzene Derivatives*.
24. Krishnakumar V, Prabavathi N (2008) Simulation of IR and Raman spectral based on scaled DFT force fields: a case study of 2-amino 4-hydroxy 6-trifluoromethylpyrimidine, with emphasis on band assignment. *Spectrochim Acta A Mol Biomol Spectrosc* 71: 449-457.
25. AltunK, Golcuk K, Kumru M (2003) Structure and vibrational spectra of p-methylaniline: Hartree-Fock, MP2 and density functional theory studies. *Journal of Molecular structure (Theochem)* 637: 155.
26. Singh SJ, Pandey SM (1974) *Indian Journal of Pure and applied physics* 12: 300-305.
27. Krishna kumar V, John Xavier R (2003) *Indian Journal of Pure and applied physics* 41: 95-99.
28. Sathyanarayana DN (2003) *vibrational spectroscopy theory and applications*, 2nd edition, New Age International (P) limited publisher, New Delhi, India.
29. Kalsi PS (2003) *Spectroscopy of Organic Compounds* Wiley Eastern Limited, New Delhi, India.
30. Peesole RL, Shield LD, Mcwillam IC (1976) *modern methods of chemical analysis*, wiley, New York, USA.
31. Prabakaran AR, Mohan S (1989) *Indian Journal of Physics* 63B :468-473.
32. Sundaraganesan N, Ilakiamani S, Saleem H, Wojciechowski PM, Michalska D (2005) FT-Raman and FT-IR spectra, vibrational assignments and density functional studies of 5-bromo-2-nitropyridine. *Spectrochim Acta A Mol Biomol Spectrosc* 61: 2995-3001.
33. Sathyanarayana DN (2004) *Vibrational spectroscopy theory and application*, 2nd edition, New Age International (P) Limited publishers, New Delhi, India.
34. George S (2001) *Infrared and Raman characteristics group frequencies Tables and charts*, 3rd edition, wiley, chichester.
35. Krishnakumar V, Balachandran V (2005) FTIR and FT-Raman spectra, vibrational assignments and density functional theory calculations of 2,6-dibromo-4-nitroaniline and 2-(methylthio)aniline. *Spectrochim Acta A Mol Biomol Spectrosc* 61: 1811-1819.
36. Kanna Rao RA, Syam Sunder N (1993) Vibrational spectra of 2-fluoro-5-nitro-, 2-fluoro-4-nitro-, 4-fluoro-2-nitro- and 5-fluoro-2-nitrotoluene. *Spectrochimica Acta* 49A: 1691.
37. Silverstein M, Basseler GC, Morill C (1981) *Spectrometric Identification of Organic Compounds*, Wiley, New York, USA.
38. Jag Mohan (2000) *Organic Spectroscopy Principles and Applications*, Narosa Publishing House, New Delhi, India.
39. Bowman WD, Spiro TG (1980) *Journal of Chemical Physics* 73: 5482.
40. Sundaraganesan N, Joshua BD (2007) Vibrational spectra and fundamental structural assignments from HF and DFT calculations of methyl benzoate. *Spectrochim Acta A Mol Biomol Spectrosc* 68: 771-777.
41. Watanabe T, Ebata T, Tanabe S, Mikami N (1996) *Journal of Chemical Physics* 105: 408-412.
42. Coates J (2000) Interpretation of infrared spectra, a practical approach, in: R.A. Meyersin *Encyclopedia of Analytical Chemistry*, John Wiley & Sons Ltd., Chichester.
43. Ahmad S, Mathew S, Verma PK (1992) *Indian Journal of Pure and Applied Physics* 30: 764-770.
44. Vander Maas JH and Lutz ETG (1974) Structural information from OH stretching frequencies monohydric saturated alcohols. *Spectrochimica Acta* 30A: 2005-2019
45. Ahmad S, Mathew S, Verma PK (1992) *Indian Journal of Pure and Applied Physics* 30: 764-770.
46. Gorelsky SI, Wizard S Program Revision 4.5, University of Ottawa, Ottawa, Canada.